DISTILAT
Jurnal Teknologi Separasi

Distilat. 2024, 10 (4), 950-960
p-ISSN : 1978-8789, e-ISSN : 2714-7649
http://jurnal.polinema.ac.id/index.php/distilat
DOI: https://doi.org/10.33795/distilat.v10i4.6651

HIGH-ENERGY MILLING OF MAGNESIUM WITH ZEOLITE FOR HYDROGEN STORAGE

Adhira Satria Pratama[1, 3], Gumawa Windu Manggada[2], Magdy Abdelghany Elsayed[2], and Shixue Zhou[3]

[1]Department of Chemical Engineering, Politeknik Negeri Malang, Jl. Soekarno Hatta No. 9, Malang 65141, Indonesia

[2]College of Energy and Mining Engineering, Shandong University of Science and Technology, 579 Qianwangang Road, Qingdao 266590, China

[3]College of Chemical and Biological Engineering, Shandong University of Science and Technology, 579 Qianwangang Road, Qingdao 266590, China

adhirasatria123@gmail.com; [zhoushixue66@163.com]

ABSTRACT

Magnesium has received great attention as a potential material for hydrogen storage due to its environmental friendliness, high gravimetric hydrogen storage capacity, and low cost. However, the material's effectiveness is limited by its high thermodynamic stability, which makes hydrogen desorption challenging, and low reaction kinetics, which slows the rate of hydrogen absorption and desorption. To enhance the performance of magnesium as a hydrogen storage material, this work innovatively aims to examine the impact of time and high energy milling speed on particle size as well as the milling aid effect of zeolite 5A. Experiment results showed that after ball milling with 4 h milling time and 270 r/min milling speed, the size of magnesium crystallites calculated from XRD data is in the range of 32.8-49.3 nm, while the size before ball milling was 72.7 nm. The kinetic measurement results showed that the Mg+10 wt.% zeolite 5A+10 wt.% Ni sample with 4 h milling time and 270 r/min milling speed at 330°C and 2.5 MPa had the best absorption and desorption capacity of 4.14 wt.% and 3.91 wt.%, respectively, in less than 25 min. The synergistic effect of milling time, milling speed, and the addition of zeolite 5A with Ni has a significant role in reducing the size of Mg particles, which affects the absorption and desorption performance of magnesium.

Keywords: *absorption, desorption, high energy milling, hydrogen storage, zeolite.*

1. INTRODUCTION

Currently, fossil fuels are the main energy source for driving vehicles. However, there will be an energy problem because these resources are finite. Natural gas and coal supplies will run out in 70 to 200 years at present usage rates, while petroleum reserves are predicted to run out sooner [1, 2]. Hydrogen is one of the best candidates to replace fossil fuels because it is environmentally friendly since it has the highest energy density per unit mass (120 MJ/kg), is easily converted into electricity, and is abundant on earth [3-5]. The challenge of using hydrogen as a commercial fuel is to store hydrogen safely and efficiently [6, 7]. To fully realize the potential of the hydrogen economy, researchers investigated different methods for hydrogen storage. They identified three primary ways to store hydrogen, each with specific

Corresponding author: Shixue Zhou
College of Chemical and Biological Engineering, Shandong University of Science and Technology
579 Qianwangang Road, Qingdao 266590, China
E-mail: zhoushixue66@163.com

benefits. First, hydrogen was stored as a compressed gas in high-pressure tanks, which could withstand pressures up to 80 MPa. Second, it was stored as a liquid in tanks maintained at extremely low temperatures of -253°C. Finally, hydrogen was stored in solid-state forms through absorption, adsorption, and chemical reactions with metals or other compounds [8-10].

Mg-based hydride materials are widely used for hydrogen storage applications because they have the highest hydrogen capacity of 7.6 wt.%, a mass-energy density of 2600 Wh/kg, and a volumetric energy density of 3700 Wh/L [11-13]. However, the thermodynamic and kinetic performance of magnesium hydride is poor due to the strong bond energy of the Mg-H bond, resulting in a high decomposition temperature. This happens because, as magnesium hydride starts to form on the surface of magnesium powder during the hydrogenation process, it rapidly develops a layer of magnesium hydride on the surface [14].

Tailoring the microstructure and crystal structure of the alloy, such as grain size, can also affect the hydrogen absorption and desorption performance of magnesium alloys [15]. The atomic density of magnesium can be reduced by reducing the crystallite size or refining the grain size of the hydrogen storage material [16, 17]. Magnesium alloys and their composites are the most frequently used materials to store hydrogen in its solid state [18]. Alloying is a method used to improve the thermodynamic properties and kinetics of hydrogen absorption. It was discovered that the thermodynamic and kinetic characteristics of hydrogen absorption can be enhanced by alloying Mg with Ni, Al, Cu, Fe, and Si by reducing the stability of Mg–H bonds, thereby lowering the temperature required for hydrogen absorption and desorption, and by introducing catalytic sites and lattice defects that accelerate hydrogen diffusion and facilitate faster reaction rates. For example, Mg-Co and Mg-Ni have kinetics much better than pure Mg [19-21]. Among Mg-based alloys, Mg_2Ni is one of the most promising magnesium-based alloys for hydrogen storage because of its advantageous thermodynamics and comparatively high hydrogen capacity. Following hydrogenation at moderate temperatures, Mg_2Ni transforms into the ternary hydride Mg_2NiH_4, with a with a hydrogen capacity of 3.6 wt.% [22, 23].

Zeolites has the characteristics of chemical and thermal stability, high internal surface area, microporous structure, renewability, and cost-effectiveness [24, 25]. Zeolites enhance hydrogen storage performance by effectively dispersing hydrogen storage materials; for example, MgH_2 combined with zeolite SAPO-34 achieves a hydrogen content of approximately 6.08 wt.% [26]. This work utilized high-energy ball milling to prepare magnesium with zeolite 5A and Ni, characterized its morphology using X-ray diffraction (XRD), and evaluated its hydrogen absorption and desorption kinetics via a pressure composition temperature machine (PCT). It innovatively examines the influence of milling time and speed on particle size, analyzing the enhancement of magnesium as a hydrogen storage material with zeolite 5A.

2. RESEARCH METHODS

2.1. Raw materials

In this work, we utilized high-purity materials from various suppliers. Magnesium (>99.9% purity) was sourced from Tianjin Ruijinte Chemical Co., Ltd. Zeolite 5A (>99.9% purity) was obtained from Sigma-Aldrich (233676). Nickel powder (>99.5% purity) came

from Beijing Hua Wei Rui Ke Chemical Co., Ltd. High-purity gases were also used: hydrogen (>99.999% purity), nitrogen (>99.999% purity), and argon (>99.999% purity), all supplied by Qingdao Deyi Gas Co., Ltd.

2.2. Preparation of materials

High-energy milling to prepare hydrogen storage materials was conducted using a planetary ball mill (ND7 model, Nanda Tianzun Instrument Company, China) in two categories. The first operated with two samples (Mg + 10 wt.% zeolite 5A + 10 wt.% Ni and Mg + 30 wt.% zeolite 5A + 10 wt.% Ni) at 30 Hz (180 r/min) for 2 h, with a cooling period of 5 min every 20 min to mitigate heat generated by the zirconia balls as a grinding medium. The second was conducted with two samples (Mg + 10 wt.% zeolite 5A + 10 wt.% Ni and Mg + 30 wt.% zeolite 5A + 10 wt.% Ni) at 45 Hz (270 r/min) for 4 h, employing the same cooling intervals as the first category.

2.3. Analysis and Characterization Techniques

X-ray diffraction (XRD) was performed on an Ultima IV multi-functional level X-ray diffractometer operating at a scanning speed of 8 deg./min. X-ray diffraction occurs when monochromatic X-ray beams interact with the surface of a crystalline material. These X-rays are generated by bombarding a Cu target with electrons emitted from a heated tungsten filament, resulting in $Cu\ K_\alpha$radiation due to ionization. The sample is irradiated at a controlled incident angle, causing diffraction patterns from its crystallographic planes. With particle sizes in the powder less than 100 nm, internal particle stress is negligible, allowing accurate determination of crystal phase sizes using the Scherrer equation (1) [27].

$$Lc = \frac{k\lambda}{\beta cos\ \theta} \quad (1)$$

Where Lc is the crystallite size in nm; k is a dimensionless shape factor, and its value is 0.89. λ is the wavelength of the Cu $K_{\alpha1}$ radiation, 0.154056 nm; β is the full-width at half maximum (FWHM) in rad.; θ is the peak diffraction angle in rad. The obtained XRD patterns were analyzed by Jade 6.0 software (Materials Data Inc.) to determine the crystal phase composition, interplanar spacing, crystallite size, and unit cell parameters.

2.4. Kinetic Analysis

The hydrogen absorption and desorption kinetics were measured by the automatic sievert's type apparatus (PCTPro-2000, Setaram, France). Samples identified in Section 2.2 were weighed in a glovebox and then placed into the sample cell. A heating jacket was used to maintain consistent temperatures during the experiment. Each sample was evacuated for 20 minutes to establish initial conditions. Parameters for hydrogen absorption and desorption pressures in the reservoirs, as well as experimental temperature and cycle settings, were accurately set before conducting the experiments. For the Mg-5A-Ni composites, the specific weight of the sample was analyzed per measurement. Kinetic curves were obtained at three different temperatures, 270°C, 300°C, and 330°C, for hydrogen absorption with an initial pressure of 2.5 MPa and desorption with an initial pressure of 0.001 MPa.

3. RESULTS AND DISCUSSION

3.1 Crystal structure of the materials

X-ray diffraction was conducted on pure Mg, Mg with 10 wt.% zeolite 5A and 10 wt.% Ni after 2 h and 4 h of milling, and Mg with 30 wt.% zeolite 5A and 10 wt.% Ni after 2 h and 4 h of milling. Figure 1 displays the XRD patterns comparing these samples under different milling conditions; (a) pure Mg; (b) Mg + 10 wt.% zeolite 5A + 10 wt.% Ni with a milling speed of 30 Hz and 2 h of milling time; (c) Mg + 30 wt.% zeolite 5A + 10 wt.% Ni with the same milling parameters. Additionally, (d) shows Mg + 10 wt.% zeolite 5A + 10 wt.% Ni and (e) Mg + 30 wt.% zeolite 5A + 10 wt.% Ni, respectively, milled at 45 Hz for 4 h. The XRD analysis performed using Jade 6.0 revealed distinct patterns for five different samples.

Before milling, the XRD analysis of the magnesium sample in Figure 1 (a) reveals a crystalline structure characterized by prominent diffraction peaks corresponding to various crystallographic planes. The unit cell parameter is 3.2 Å × 3.2 Å × 5.2 Å, indicating the dimensions of the crystal lattice. Notably, the (101) crystal face exhibits a strong diffraction peak at 36.4° of 2θ with 100% intensity and area, indicating its prevalence in the sample (Table 1). Other significant peaks include (002) at 34.2° and (100) at 31.9°, showing substantial intensities and areas as well. The crystallite sizes, ranging from 63.6 nm to 91.1 nm as determined by peak broadening, suggest a heterogeneous distribution of crystallite sizes within the sample. These findings collectively describe the crystalline nature and crystallite characteristics of the magnesium sample before any milling processes.

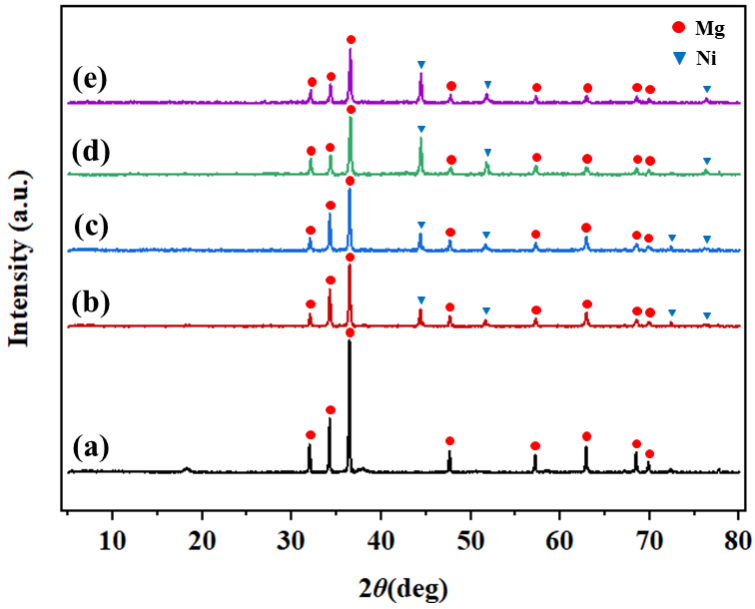

Figure 1: XRD patterns of magnesium before and after milling with zeolite 5A and Ni. Mg before milling (a); Mg + 10 wt.% zeolite 5A + 10 wt.% Ni, 30 Hz, 2 h (b); Mg + 30 wt.% zeolite 5A + 10 wt.% Ni, 30 Hz, 2 h (c); Mg + 10 wt.% zeolite 5A + 10 wt.% Ni, 45 Hz, 4 h (d); Mg + 30 wt.% zeolite 5A + 10 wt.% Ni, 45 Hz, 4 h (e).

Table 1. XRD analysis results for magnesium powder before milling

Crystal face	2Θ (◦)	Intensity (%)	Area (%)	Crystallite size (nm)
(100)	31.9	20.7	20.5	72.4
(002)	34.2	40.8	36.0	91.1
(101)	36.4	100.0	100.0	71.9
(110)	57.2	12.7	14.4	63.6
(103)	62.9	19.2	21.4	67.1
(200)	68.4	15.4	17.0	70.5

The XRD data presented in Table 2 outlines the diffraction characteristics of magnesium samples modified with zeolite (5A) and nickel (Ni) under different compositions and milling conditions. Each entry corresponds to a specific sample configuration, detailing the crystal face observed, the 2θ angle of diffraction, the intensity of the peaks relative to the strongest peak, the area under each peak, and crystal size. For instance, samples labeled (b) and (c) (Figure 1) were magnesium combined with 10 wt.% and 30 wt.% zeolite (5A), respectively, and were subjected to milling at 30 Hz for 2 h. In these samples, the (002) crystal face shows varying intensities and areas; sample (b) exhibits an intensity of 59.1% and an area of 63.1%, while sample (c) shows an intensity of 55.8% and an area of 55.4%. These differences suggest variations in crystallographic orientation or crystallite size distribution within the samples. Furthermore, comparing samples under different milling conditions reveals additional insights. For example, samples (d) and (e) (Figure 1) maintain the composition of 10 wt.% and 30 wt.% zeolite 5A, respectively, but were milled at a higher frequency 45 Hz for a longer duration 4 h. Interestingly, the (002) peak in sample (d) at 34.3° shows a distinct intensity of 32.4% and an area of 26.6%, while sample (e) exhibits an intensity of 34.1% and an area of 35.2% at the same angle. This suggests that the milling conditions influence not only the intensity but also the crystallite size or preferred orientation of the magnesium phases. The effect of ball milling on crystal size is intricately influenced by several key factors, such as raw material composition, milling time, and milling speed. Introducing zeolite 5A alongside Ni into the Mg matrix has shown a consistent trend towards smaller crystal sizes, attributed to enhanced nucleation and milling efficiency facilitated by the zeolite particles. Increasing milling time from 2 to 4 h has consistently led to reduced crystallite sizes, as prolonged milling allows for more thorough particle refinement through increased collisions and interactions. Similarly, higher milling speeds, exemplified by an increase from 30 Hz to 45 Hz, have been shown to further decrease crystallite sizes due to intensified milling forces and more efficient particle size reduction.

Overall, the XRD data provides a detailed characterization of how varying the composition of zeolite 5A and Ni in magnesium, along with different milling parameters, affects the structural properties of the samples. These data are important for understanding the crystalline behavior and optimizing the synthesis conditions for applications requiring specific material properties, such as catalysis or structural reinforcement.

Table 2. Milling conditions and XRD analysis results of different composite materials

Zeolite 5A (%)	Time (h)	Speed (r/min)	Crystal face	2Θ (◦)	Intensity (%)	Area (%)	Crystallite size (nm)
10[(b)]	2	180	(100)	32.0	19.5	20.2	47.2
			(002)	34.2	59.1	63.1	49.3
			(101)	36.4	100.0	100.0	44.2
30[(c)]	2	180	(100)	32.0	22.3	22.7	43.7
			(002)	34.2	55.8	55.4	44.0
			(101)	36.4	100.0	100.0	42.5
10[(d)]	4	270	(100)	32.1	27.7	27.9	36.2
			(002)	34.3	32.4	26.6	38.2
			(101)	36.5	100.0	100.0	32.8
30[(e)]	4	270	(100)	32.1	22.5	19.3	35.5
			(002)	34.3	34.1	35.2	41.2
			(101)	36.5	100.0	100.0	34.8

3.2 Kinetic Measurement

a. Hydrogen kinetics on Mg + 10 wt.% zeolite 5A + 10 wt.% Ni composite milled at 30 Hz for 2 h

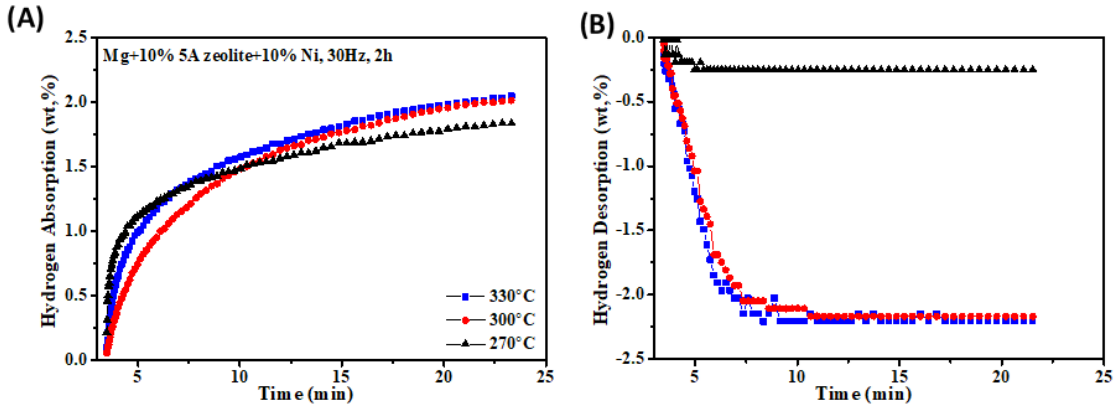

Figure 2. Hydrogen absorption (A) and desorption (B) on Mg + 10 wt.% zeolite 5A + 10 wt.% Ni composite, milled at 30 Hz for 2 h, at different temperatures.

Figure 2 displays the hydrogen absorption and desorption of a composite material of Mg with 10 wt.% zeolite 5A and 10 wt.% Ni, milled at 30 Hz for 2 h. Figure 2 (A) shows hydrogen absorption over time at three different temperatures: 330°C (blue squares), 300°C (red circles), and 270°C (black triangles). Absorption increases with time, reaching higher levels at elevated temperatures. At 330°C, the absorption capacity reaches approximately 2.05 wt.% within 25 min, whereas at 300°C, it reaches around 2.01 wt.%, and at 270°C, it reaches about 1.83 wt.%. Figure 2 (B) indicates hydrogen desorption over time, revealing a rapid initial desorption phase that slows down and plateaus. At 330°C, the desorption quickly drops to about 2.01 wt.% within the first 5 min; at 300°C, it drops to around 1.81 wt.%; and at 270°C, it shows minimal desorption equal to 0.25 wt.%. These results demonstrate that the hydrogen storage capacity and kinetics are temperature-

dependent, with higher temperatures improving both absorption and desorption processes.

b. Hydrogen kinetics on Mg + 30 wt.% zeolite 5A + 10 wt.% Ni composite milled at 30 Hz for 2 h

In Figure 3 (A), the absorption increases with time, reaching higher levels at elevated temperatures. At 330°C, the absorption capacity reaches approximately 1.82 wt.% within 25 min, whereas at 300°C, it reaches around 0.66 wt.%, and at 270°C, it reaches about 0.40 wt.%. Figure 3 (B) shows hydrogen desorption over time, revealing a rapid initial desorption phase that slows down and plateaus. At 330°C, the desorption quickly drops to about 0.83 wt.% within the first 5 min; at 300°C, it drops to around 0.53 wt.%; and at 270°C, it shows minimal desorption. Comparing these results with the previous figure, where the composite contained 10 wt.% 5A zeolite, we observe that increasing the 5A zeolite content to 30 wt.% results in a slightly lower absorption capacity at the highest temperature (1.82 wt.% vs 2.01 wt.% at 330°C). However, the general trend of increased absorption and desorption at higher temperatures remains consistent. The desorption rates are also lower in the current composite, indicating that the higher zeolite content may be affecting the kinetics of hydrogen release. Overall, the composite with higher zeolite content shows lower absorption and desorption capacities compared to the one with 10 wt.% 5A zeolite.

c. Hydrogen kinetics on Mg + 10 wt.% zeolite 5A + 10 wt.% Ni composite milled at 45 Hz for 4 h

After milling at 45 Hz for 4 h, at 330°C, the absorption capacity is about 4.14 wt.% in less than 25 min, whereas at 300°C, it is about 3.89 wt.%, and at 270°C, it is about 3.60 wt.% Figure 4 (A). Figure 4 (B) shows the hydrogen desorption capacity at temperatures of 270°C, 300°C, and 330°C, hydrogen desorption is about 1.04 wt.%, 3.74 wt.%, and 3.91 wt.%.

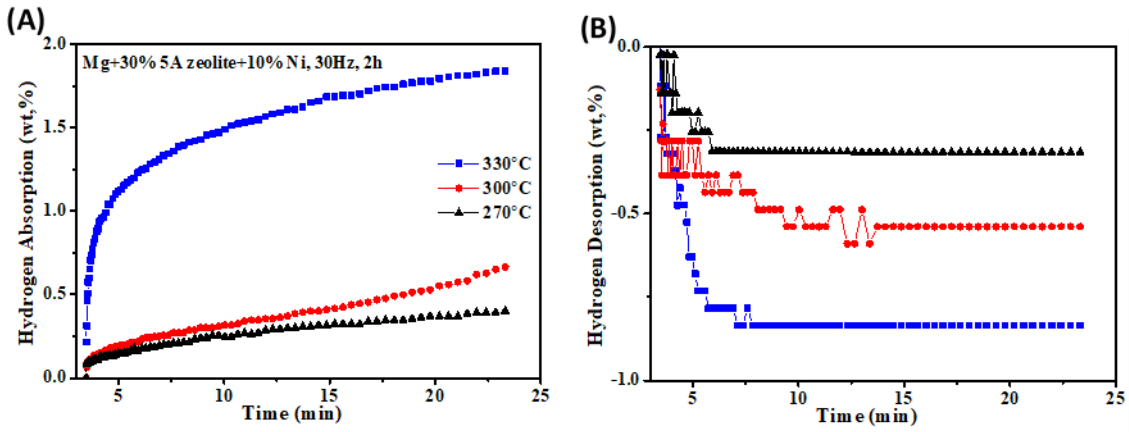

Figure 3. Hydrogen absorption (A) and desorption (B) on Mg + 30 wt.% zeolite 5A + 10 wt.% Ni composite, milled at 30 Hz for 2 h, at different temperatures.

Figure 4 shows that increasing the milling frequency to 45 Hz and duration to 4 h significantly enhances hydrogen absorption and desorption capacities. This indicates that more intensive milling conditions (higher frequency and longer duration) improve both the absorption and desorption performance of the composite material.

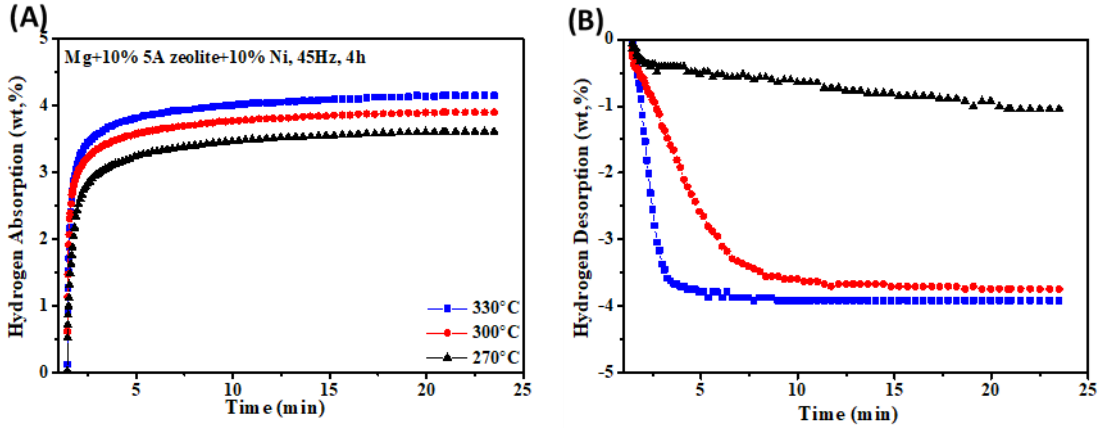

Figure 4. Hydrogen absorption (A) and desorption (B) on Mg + 10 wt.% zeolite 5A + 10 wt.% Ni composite, milled at 45 Hz for 4 h, at different temperatures.

d. Hydrogen Kinetic on Mg + 30 wt.% zeolite 5A + 10 wt.% Ni composite milled at 45 Hz for 4 h

The results in Figure 5 (A) show that the amount of hydrogen absorbed by these composite increases with temperature, specifically 0.40 wt.% at 270°C, 1.83 wt.% at 300°C, and 2.62 wt.% at 330°C. The temperature-dependent increase indicates that higher temperatures facilitate greater hydrogen absorption. Figure 5 (B) shows the hydrogen desorption capacity at temperatures of 270°C, 300°C, and 330°C, hydrogen desorption is about 0.53 wt.%, 0.83 wt.%, and 2.64 wt.%. Comparing these results with other composite formulations tested Mg + 30 wt.% zeolite 5A + 10 wt.% Ni composites (milled at 45 Hz for 4 h) show high hydrogen storage performance at elevated temperatures compared to Mg + 10 wt.% zeolite 5A + 10 wt.% Ni composites (milled at 30 Hz for 2 h) and Mg + 30 wt.% zeolite 5A + 10 wt.% Ni composites (milled at 30 Hz for 2 h). However, they exhibit lower performance compared to Mg + 10 wt.% zeolite 5A + 10 wt.% Ni composites (milled at 45 Hz for 4 h). These data underscore the important influence of composition and milling parameters on hydrogen storage composites. The determination of these factors is essential for enhancing the efficiency and effectiveness of these materials in practical hydrogen storage applications. The Mg + 10 wt.% zeolite 5A + 10 wt.% Ni composites, processed with 45 Hz milling for 4 h, exhibit promising hydrogen absorption capabilities across a range of temperatures. This optimized method significantly increases surface area and enhances exposure to active sites, suggesting promising potential for efficient applications in hydrogen storage. This composite is an ideal material for advanced hydrogen storage systems, such as automotive fuel cells, which require lightweight, efficient storage and fast refueling. In addition, this composite can provide benefits for renewable energy storage systems that require safe and efficient hydrogen storage solutions.

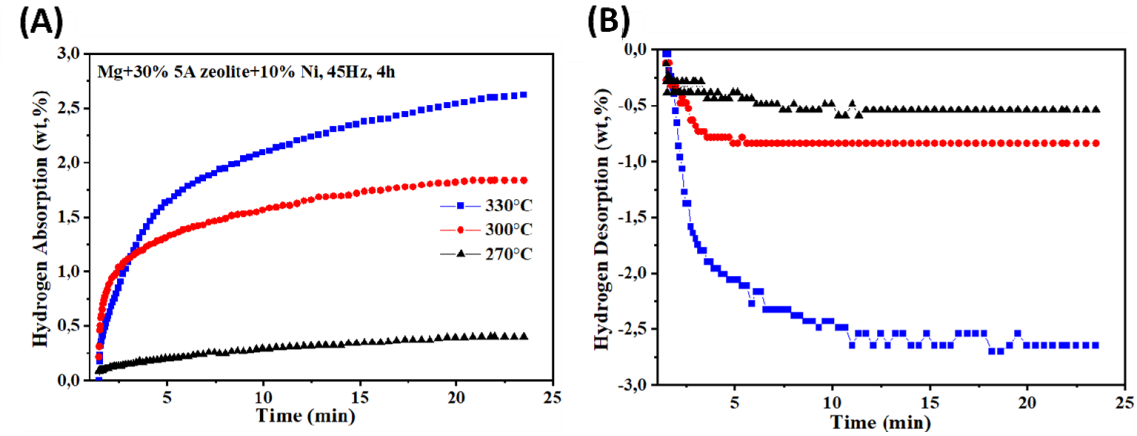

Figure 5. Hydrogen absorption (A) and desorption (B) on Mg + 30 wt.% zeolite 5A + 10 wt.% Ni composite, milled at 45 Hz for 4 h, at different temperatures.

4. CONCLUSION AND SUGGESTIONS

This article investigated the hydrogen storage properties of magnesium milled with zeolite 5A and Ni. X-ray diffraction analysis revealed a significant reduction in crystallite size across all samples. Specifically, the crystallite size of magnesium decreased from 71.9 nm before milling to a range of 32.8-49.3 nm after ball milling under various conditions of milling time, milling speed, and zeolite 5A ratios. Zeolite 5A functioned as a dispersing agent and cracking agent during ball milling, effectively contributing to the further reduction in magnesium crystal size. In addition, the hydrogen absorption and desorption kinetic properties of Mg + zeolite 5A + Ni samples with different milling times, speeds, and ratios have also been studied. The composite of Mg + 10 wt.% zeolite 5A + 10 wt.% Ni, processed by 45 Hz milling for 4 h, showed promising hydrogen absorption capacity reaching 4.14 wt.% and desorption reaching 3.91 wt.% at 330°C. The results indicated that they were much higher than the other samples.

Further research on magnesium-based hydrogen storage materials should focus on several key aspects, including optimizing the milling time and increasing the milling speed. These factors significantly affect the particle size reduction, which can improve the adsorption and desorption capabilities of hydrogen storage materials. The addition of Zeolite 5A effectively aids in reducing the size of the material, but excessive quantities can negatively impact the hydrogen absorption and desorption performance.

ACKNOWLEDGEMENT

This work was financially supported by the National Natural Science Foundation of China (21978156). All the authors would like to express their sincere gratitude and appreciation for National Natural Science Foundation of China.

REFERENCES

[1] J. Ren, N. M. Musyoka, H. W. Langmi, M. Mathe, S. Liao, “Current research trends and perspectives on materials-based hydrogen storage solutions: A critical review”, *International Journal of Hydrogen Energy*, vol. 42, hal. 289-311, 2017.

[2] X. Xie, M. Chen, M. Hu, B. Wang, R. Yu, T. Liu, "Recent advances in magnesium-based hydrogen storage materials with multiple catalysts", *International Journal of Hydrogen Energy*, vol. 44, hal. 10694-10712, 2019.

[3] A. Kundu, R. Trivedi, N. Garg, B. Chakraborty, "Novel permeable material yttrium decorated zeolite templated carbon for hydrogen storage: Perspectives from density functional theory", *International Journal of Hydrogen Energy*, vol. 47, hal. 28573-28584, 2022.

[4] M. R. Usman, "Hydrogen storage methods: Review and current status", *Renewable and Sustainable Energy Reviews*, vol. 167, 2022.

[5] A. Gupta, G. V. Baron, P. Perreault, S. Lenaerts, R. G. Ciocarlan, P. Cool, "Hydrogen clathrates: next-generation hydrogen storage materials", *Energy Storage Materials*, vol. 41, hal. 69-107, 2021.

[6] S. Al, N. Cavdar, N. Arikan, "Computational evaluation of comprehensive properties of MgX_3H_8 (X = Sc, Ti, and Zr) as effective solid state hydrogen storage materials" , *Journal of Energy Storage*, vol. 80, hal. 110402, 2024.

[7] Z. Wang, Z. Tian, P. Yao, H. Zhao, C. Xia, T. Yang, "Improved hydrogen storage kinetic properties of magnesium-based materials by adding Ni_2P", *Renew Energy*, vol. 189, hal. 559-569, 2022.

[8] A. Kumar, P. Muthukumar, P. Sharma, and E. A. Kumar, "Absorption-based solid-state hydrogen storage system: A review", *Sustainable Energy Technologies and Assessments*, vol. 52, hal. 102204, 2022.

[9] Y. Qi, P. Sheng, H. Sun, J. Li, W. Zhang, S. Guo, D. Zhao, Y. Zhang, "Hydrogen storage thermodynamics and kinetics of the as-cast and milled Ce-Mg-Ni-based alloy", *Materials Today Communications*, vol. 35, hal. 106217, 2023.

[10] Y. Shang, C. Pistidda, G. Gizer, T. Klassen, M. Dornheim, "Mg-based materials for hydrogen storage", *Journal of Magnesium and Alloys*, vol. 9, hal. 1837-1860, 2021.

[11] Q. Luo, J. Li, B. Li, B. Liu, H. Shao, Q. Li, "Kinetics in Mg-based hydrogen storage materials: Enhancement and mechanism", *Journal of Magnesium and Alloys*, vol. 7, hal. 58-71, 2019.

[12] Y. Sui, Z. Yuan, D. Zhou, T. Zhai, X. Li, D. Feng, Y. Li, Y. Zhang, "Recent progress of nanotechnology in enhancing hydrogen storage performance of magnesium-based materials: A review", *International Journal of Hydrogen Energy*, vol. 47, hal. 30546-30566, 2022.

[13] S. J. Huang, M. P. Mose, "High-energy ball milling-induced crystallographic structure changes of AZ61-Mg alloy for improved hydrogen storage", *Journal of Energy Storage*, vol. 68, hal. 107773, 2023.

[14] K. Alsabawi, T. A. Webb, E. M. A. Gray, C. J. Webb, "Kinetic enhancement of the sorption properties of MgH_2 with the additive titanium isopropoxide", *International Journal of Hydrogen Energy*, vol.42, hal. 5227-5234, 2017.

[15] Y. Qi, P. Sheng, J. Li, X. Zhang, W. Zhang, S. Guo, Y. Zhang, "Improved hydrogen storage thermodynamics and kinetics of La-Ce-Mg-Ni alloy by ball milling", *Journal of Physics and Chemistry of Solids*, vol. 179, hal. 111417, 2023.

[16] Y. Liu, Y. Guo, Y. Jiang, L. Feng, Y. Sun, and Y. Wang, "Recent progress in thermodynamic and kinetics modification of magnesium hydride hydrogen storage materials", *Materials Reports: Energy*, vol. 4, hal. 100252, 2024.

[17] Z. Ding, Y. Li, H. Yang, Y. Lu, J. Tan, J. Li, Q. Li, Y. Chen, L. L. Shaw, F. Pan, "Tailoring MgH_2 for hydrogen storage through nanoengineering and catalysis", *Journal of Magnesium and Alloys*, vol. 10, hal. 2946-2967, 2022.

[18] N. Kumar, S. Soren, "Magnesium metal nano composites- A solid state hydrogen storage material", *Mater Today Proc*, 2023.

[19] E. H. Abdechafik, H. A. Ousaleh, S. Mehmood, Y. F. Baba, I. Burger, M. Linder, A. Faik, "An analytical review of recent advancements on solid-state hydrogen storage", *International Journal of Hydrogen Energy*, vol. 52, hal. 1182-1193, 2024.

[20] X. Li, Z. Yuan, C. Liu, Y. Sui, T. Zhai, Z. Hou, Z. Han, Y. Zhang, "Research progress in improved hydrogen storage properties of Mg-based alloys with metal-based materials and light metals", *International Journal of Hydrogen Energy*, vol. 50, hal. 1401-1417, 2024.

[21] Y. Xu, Y. Deng, W. Liu, X. Zhao, J. Xu, Z. Yuan, "Research progress of hydrogen energy and metal hydrogen storage materials," *Sustainable Energy Technologies and Assessments*, vol. 55, hal. 102974, 2023.

[22] J. Wen, P. de Rango, N. Allain, L. Laversenne, T. Grosdidier, "Improving hydrogen storage performance of Mg-based alloy through microstructure optimization," *Journal Power Sources*, vol. 480, 2020.

[23] A. Gupta, M. Faisal, A. Flamina, R. M. Raghavendra, F. Hassan, N. Kundan, N. Kumar, "Enhanced hydrogen storage in Mg catalysed by Cu–Ni–Co–Fe quaternary multi-component alloy," *International Journal Hydrogen Energy*, vol. 50, hal. 932-945, 2024.

[24] T. Hai, F. A. Alenizi, A. H. Mohammed, B. S. Chauhan, B. Al-Qargholi, A. S. M. Metwally, M. Ullah, "Machine learning-aided modeling of the hydrogen storage in zeolite-based porous media," *International Communications in Heat and Mass Transfer*, vol. 145, 2023.

[25] Z. Ozturk, "Hydrogen storage on lithium modified silica-based Chabazite type zeolite, A computational study," *International Journal Hydrogen Energy*, vol. 43, hal. 22365-22376, 2018.

[26] S. Xi, X. Wang, K. Caren, T. Zhang, Z. Han, M. Gao, S. Zhou, H. Yu, "Effect of Ni and SAPO-34 co-additive on enhancing hydrogen storage performance of MgH2", *International Journal Hydrogen Energy*, vol. 46, no. 46, hal. 23748-23756, 2021.

[27] Y. S. Chuang and S. J. Hwang, "Synthesis and hydrogen absorption/desorption properties of Mg-Nb2O5-SWCNT/MWCNT nanocomposite prepared by reactive milling," *Journal of Alloy and Compounds*, vol. 656, hal. 835-842, 2015.